

Magnetic diffusion-limited aggregation

N. Vandewalle and M. Ausloos

*Services Universitaires Pour la Recherche, et les Applications en Supraconductivité, Institut de Physique B5,
Université de Liège, Sart Tilman, B-4000 Liège, Belgium*

(Received 16 September 1994)

An extra degree of freedom is introduced in the well-known diffusion-limited aggregation model. The growth entities are “spins” taking, e.g., two states that are coupled via a physically relevant interaction potential responsible for a competition process between the two components. The presence of an external field favoring one spin species over the other is also considered. This model leads to a wide variety of kinetic processes and morphologies distributed in a “phase diagram” of both growth control parameters, i.e., the coupling energy and the field strength. The Brownian motion of the spins leads to fractal-like structures with a fractal dimension varying from 1.68 ± 0.02 to 1.99 ± 0.01 depending upon the growth parameters. A physical basis is presented to describe the new kinetic processes. The spreading and geometry of the two components in fractal clusters have also been investigated. The earlier stages of growth are driven by a dominating spin component. This finite-size process is found to imply a drastic change of the physical and geometrical properties of the cluster during growth history. For large clusters the fractal branches can be divided into segments of the same spin species having a characteristic coherence length ξ . This length ξ is found numerically to scale as a power law of the segment mass with a critical exponent $\mu = 1.2 \pm 0.1$.

PACS number(s): 68.70.+w, 61.43.Hv, 61.50.Cj, 05.50.+q

I. INTRODUCTION

For the past 50 years, kinetic growth models have received a great deal of attention because of the set of universality classes in which they belong and the natural processes which they generate [1]. Growth models are studied in many domains of science such as gelation [1], percolation [2], crystal growth [3], fracture [4], sedimentation [5], or dielectric breakdown [6].

The most simple one is the Eden model [7,8]. In this model, the growth rule consists of selectively placing a particle on an unoccupied site of a lattice in the immediate neighborhood, the so-called “perimeter,” of a cluster of identical particles. A more interesting model is the “diffusion-limited aggregation” (DLA) model introduced in 1981 by Witten and Sander [9]. It generates aggregation of particles in a cluster through a Brownian motion. Diffusion limited aggregation provides a basis for understanding a large range of natural pattern formation phenomena [9–14]. Diffusion limited aggregation has led to many generalizations and is certainly the most studied of the growth models. Many questions about such kinetic growth models remain open [12]. A theoretical “physical” understanding of the DLA growth is still a challenge [13] for the future.

Usually, natural systems are, however, constituted by entities taking different states. E.g. copolymers are macromolecules made of two kinds of monomers [15]. Some bacterian cells like *salmonella* have some gene taking two states (“on” or “off”) [16]. It is, thus, of interest to generalize the kinetic growth models in order to study the

impact of a competition between *physically different entities* on the kinetic processes.

In previous work [17], we have introduced an extra degree of freedom in the classical Eden model by replacing the identical particles by scalar spins σ_i taking two states (up or down). The introduction of a competition between the two components leads to a wide variety of cluster types in presence of an external field [17]. It has also been found that both a geometrical and a physical “transition” occur in the magnetic Eden model (MEM) at the same growth parameter values [18]. These critical spreading phenomena, which are of finite-size origin, are, however, of interest because all natural systems are finite: e.g., bacterian colonies contain no more than ten thousand cells.

Recently, an interesting variant of DLA was imagined where geometrically different element aggregates, i.e., particles of different sizes, are taken into account [19]. See, also, Refs. [20] and [21]. In the latter work, sticking, rearrangement, and evaporation rates compete with each other. In all cases, models are concerned by the transition from dense branching to dendritic morphology.

The model presented here is quite different. Specifically, herein, we introduce in the DLA model an internal degree of freedom, i.e., a spin taking two states. We will show that for finite-size systems the “quenching” of the degree of freedom on the cluster leads to branching or compactness but moreover to combined geometric and physical “transitions” at size dependent critical values. Our work leads to an extension of studies on growth models and add to the wide field of localized spin statistical mechanics, and, thus, seems to open up fields and ways for studying heterogeneous growth.

In the next section, we define such a DLA model. In Sec. III, the processes and the geometrical properties of

*Electronic address: vandewal@gw.unipc.ulg.ac.be

†Electronic address: u2150ma@bliulg11.bitnet

the global shape of the clusters are studied numerically and discussed. In Sec. IV, the internal structure of the clusters and the effect of the competition is discussed with the help of numerical work. A brief discussion serves as a conclusion in Sec. V.

II. THE MAGNETIC DLA MODEL

The “magnetic diffusion-limited aggregation” (MDLA) model is defined by the aggregation of spins moving toward a cluster through a Brownian motion, as in the original DLA model. On a two-dimensional square lattice with lattice spacing a , the growth rule is defined by the following steps.

(i) An initial spin σ_0 (up or down) is dropped on a “seed site.” The extension of this monoparticle cluster is $r_{\max} = 1$.

(ii) A diffusing, up or down, spin is dropped onto a circle of radius $r_{\max} + 5a$, centered on the seed site.

(iii) A choice is then made for both the next site and the next state orientation of the diffusing spin, as the spin is allowed to flip or not flip. The probabilities of jumping to one of the four neighbor sites are defined as proportional to $\exp(-\Delta\beta E)$, where $\Delta\beta E$ is the local gain of the dimensionless Ising energy between the initial and the final states defined by

$$\beta E = -\frac{\beta J}{2} \sum_{\langle i,j \rangle} \sigma_i \sigma_j - \frac{\beta H}{2} \sum_i \sigma_i, \quad (1)$$

in which the first summation occurs only for the nearest neighbor pairs $\langle i,j \rangle$ while the second sum runs over all spins of the cluster. J and H can be considered to be an exchange integral and an external magnetic field, while β is a parameter such that βJ and βH are dimensionless. The probabilities of the eight possible configurations for each jump are renormalized and one specific configuration is chosen through a random number generator.

(iv) If the spin moves outside a circle of radius $3r_{\max}$ centered on the seed site, the spin is removed from the process and one returns to step (ii). If the spin jumps onto a perimeter site, i.e., an empty site connected to a spin of the cluster, it sticks immediately on the cluster and the next diffusing spin is launched (step ii). Then the value of r_{\max} is adapted to the largest distance between the farthest cluster site, and the seed site. However, if the spin jumps toward a neighboring site of the perimeter or to any other unconnected site, a new step (iii) is attempted.

(v) The launching and diffusing procedures are repeated until a desired number N of spins frozen on the cluster is reached.

The first term of Eq. (1) describes a short-range coupling interaction between nearest neighbor spins. This controls, in fact, the competition between the two spreading components into the clusters. The second term defines a dimensionless energy for the orientation of the spins in a magnetic field, favoring a spin species over the other one. Thus, the only two growth parameters are βJ and βH .

One should note that the motion of the diffusing spin is

Brownian when it moves toward the cluster, as for the classical DLA model. However, if the spin reaches a neighboring site of the perimeter, the diffusion is controlled by the local “magnetic” configuration on the surface of the cluster [see steps (iii) and (iv)]. The state of the alternative spin is only determined by the last step. After being glued on the cluster, a spin is not allowed to flip in order to reorganize its direction with the orientation of its neighbor spins. The growth process is irreversible and non-Markovian since the asymptotic configuration probability depends on the initial state (see also Sec. IV below).

The model could be used to simulate, or describe, electrodeposition of two atomic species, fracture of heterogeneous media, binary immiscible species, ferrofluid motion in porous media, etc.

III. GEOMETRICAL PROPERTIES OF MDLA CLUSTERS

The MDLA model conserves the essence of the classical DLA model but it presents some important differences with respect to the Witten and Sander model. Even though J and H are “energies,” the MDLA model is still a purely kinetic growth model because the diffusion and growth are driven by the probabilities $\exp(\beta J)$ and $\exp(\beta H)$. But these probabilities lead to major differences. The model takes into account semi-long-range correlations, i.e., configurations on distances longer than nearest neighbor ones. In the neighboring of the perimeter, i.e., for next nearest neighbors of the cluster sites, the sticking and diffusing probabilities already “sense” the cluster, leading to more constraints than in the DLA process [22]. One should note that 17 possible perimeter site configurations of interest are available on the two-dimensional square lattice, and that they are distributed among seven sticking probability levels, noted as P_1 to P_7 . The configurations and the associated probability levels, as function of βJ and βH , are shown in Fig. 1.

Equating the seven probability levels to each other leads to 12 linear equations between βJ and βH , with $\beta J = 0$ and $\beta H = n\beta J/2$, where n is an integer varying from -5 to 5 . (In contrast, the MEM was determined by 16 linear equations [17].) The solutions determine boundaries between 24 regions in the $(\beta J, \beta H)$ plane where the growth processes on the perimeter differ from each other. Along the $\beta J = 0$ axis, the spins are decoupled and the model simply generates the DLA process. The processes and morphologies are symmetric with respect to the $\beta H = 0$ axis. In the upper-half plane exhibited in Fig. 2, the regions are labeled AF and F for $\beta J < 0$ and $\beta J > 0$, respectively, and numbered from 1 to 6 in order of increasing field. Typical clusters of 3000 spins, simulated in the various regions of the $(\beta J, \beta H)$ diagram, are shown in Fig. 3.

In the whole ferromagnetic interaction regions $F1-F6$ of the diagram, the structure of the MDLA clusters is DLA-like but is already more extended and less side branched than a DLA cluster [see Fig. 3(b)]. In the $AF1$ region, the same cluster morphology as in $F1-F6$ regions is observed. In the $AF2$ region, the dendritic structure is

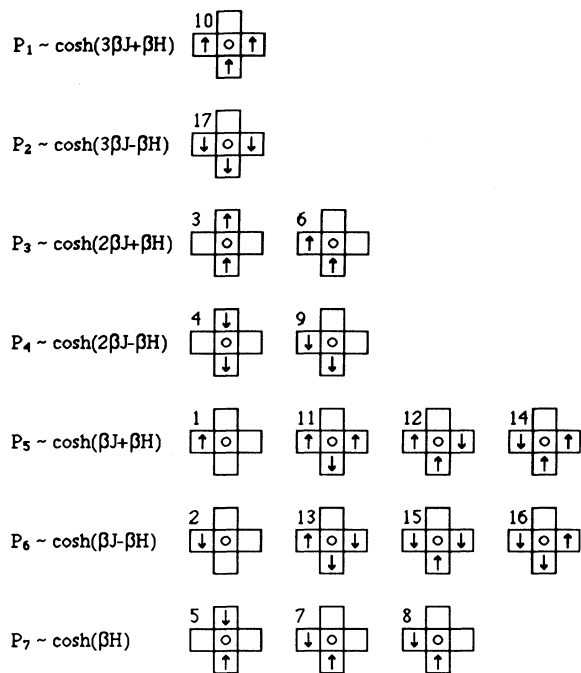


FIG. 1. Probability of sticking growth and related perimeter configurations in the 2D magnetically controlled diffusion-limited aggregation model.

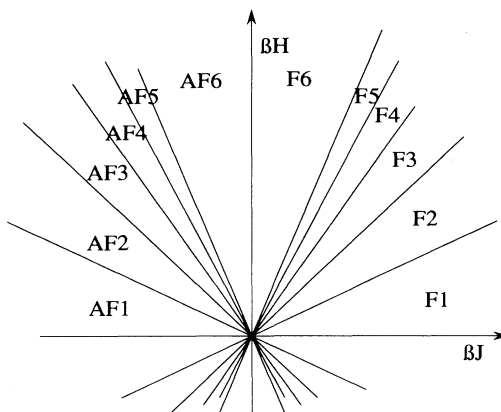


FIG. 2. Upper-half plane of the phase diagram of the magnetically controlled diffusion-limited aggregation model.

still conserved but an important thickening of the branches is observed. This thickening leads to a more moderate extension of the cluster. In the *AF3* region, compact structures are generated. However, these clusters are provided with unusual (for DLA internal lacunes and channels [see Fig. 3(e)]. In the *AF4* to *AF6* regions, “Eden treelike” (noncompact) structures [23] are generated [see Fig. 3(f)].

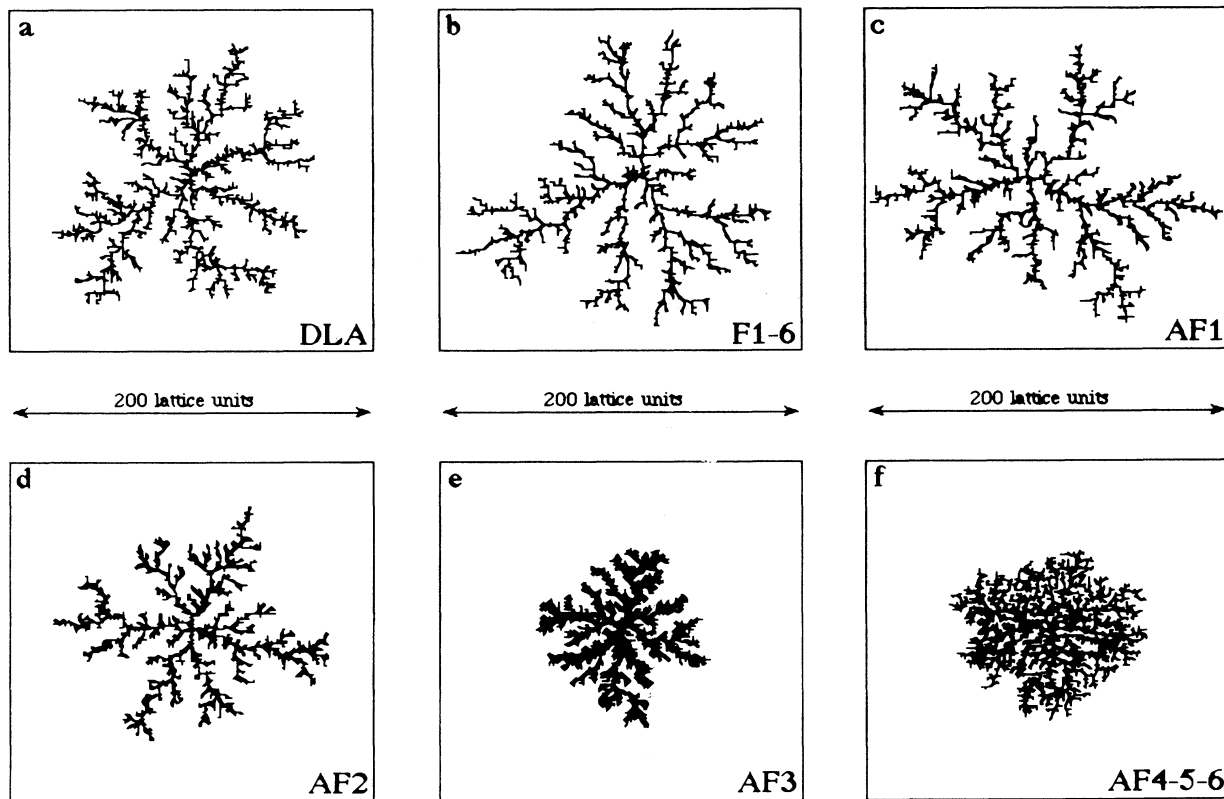


FIG. 3. Typical MDLA clusters of 3000 spins grown from an up spin as seed in various regions of the diagram of Fig. 2.

We have simulated 50 clusters of 3000 spins at various βJ and βH parameters in each region of the diagram. The cluster fractal dimension [24] is evaluated by the radius of gyration method [25]. As in the Witten and Sander simulations [9], the number of spins which has been used seems to be sufficient to give a good estimate of D_f . Fractal dimensions for each region at specific parameter values are given in Table I. We have found $D_f = 1.71 \pm 0.01$ for decoupled spins, on the βH axis. This is, of course, in good agreement with the usually reported fractal dimension of DLA clusters [9–14]. The fractal dimension D_f in the other regions takes different values ranging from 1.68 ± 0.02 to 1.99 ± 0.01 (Table I).

The cluster growth processes, as determined by the probabilities P_1 to P_7 , can be explained as follows. A magnetic field tends to enhance the effect of the positive coupling between spins because the field encourages the growth of a specific spin species. In the fjords and channels, the motion is still Brownian but in the neighborhood of the perimeter, the probability of sticking to the cluster becomes high, and, in addition, the high probability sites, close to the launching circle, are more favored than the internal sites [26,27]. This explains the structure of MDLA clusters in the ferromagnetic region, as a DLA-like structure with $D_f = 1.7$ which is approximately independent of βJ and βH . In these $F1$ - $F6$ regions, the probability P_1 always dominates the growth process.

However, in the $\beta J < 0$ region, the coupling and field effects are in conflict. This leads to a wide variety of processes and morphologies. In the $AF1$ region, the probability P_2 always dominates the growth process and leads to open antiferromagnetic-like clusters. The probability P_7 , corresponding to pure DLA growth, is the smallest one. Because the field is not high enough to break the antiferromagnetic order in the $AF1$ region, i.e., the J coupling effect dominates, the process is closely related to that which occurs in the ferromagnetic $F1$ to $F6$ regions.

In the $AF2$ region, the relevant probabilities for sticking a spin onto the cluster are different from those in $AF1$. In $AF2$, the probabilities P_5 of sticking on the tip-perimeter sites and controlling the sticking of only up spins is much smaller than the probabilities for jumping

to unconnected sites. Thus, internal perimeter sites are more favored than tip sites in the $AF2$ growth region. Configurations 4, 9, and 17, favoring down spin sticking, occur most often. This results in a thickening of the branches as seen in Fig. 3(d).

In the $AF3$ region, the probabilities of sticking close to a spin of the same species, which has been oriented in the field, are small. The diffusing spins have a tendency to wander for a long time before freezing on the cluster. The wandering appears as if the whole “surface” is visited and this leads to more compact clusters. The D_f value becomes 1.80 ± 0.02 (Table I). It is obviously quite different from the ordinary DLA value. The computing times are also very long. By decreasing βJ and staying in this region, we have noted very low sticking probabilities leading to very long computing times.

In $AF4$ to $AF6$ regions, the field dominates the coupling, and only up spin configurations are favored. The sticking probabilities, P_1 , P_3 , and P_5 are also smaller than those favoring the diffusion process. Sticking on the tip-perimeter sites, corresponding to configurations 1, 3, 6, and 10, is more favorable than sticking on other perimeter sites. This process is, thus, similar to dielectric breakdown [6] and Eden tree [23] models. We obtain the same $D_f \approx 2$ values and structures as for these models indeed.

In summary, the kinetics of DLA is found to be sensitive to the introduction of an extra degree of freedom. A wide variety of processes and obviously fractal-like structures can be, thus, generated and understood with this model.

IV. THE SPECIFIC CASE $\beta H = 0$

In this section, we study more precisely the internal competition between the two spin species when the process is driven essentially by the first term of Eq. (1), i.e., we let $\beta H = 0$ in the following. For a negative coupling βJ , an incoming spin tends to be oriented conversely to the majority orientation of its nearest neighbors in the cluster. This results in an antiferromagnetic ordering of the spins in the clusters. The two components are, however, equally distributed in the cluster [28].

On the contrary, for positive values of βJ , a ferromagnetic ordering is favored during the growth. Figure 4

TABLE I. Fractal dimension D_f of the spin clusters in the various growth regions at specific βJ - βH parameter values.

| Region | βJ | βH | D_f |
|--------|-----------|-------------------|-----------------|
| DLA | =0 | $\forall \beta H$ | 1.71 ± 0.01 |
| $F1$ | 4 | 1 | 1.70 ± 0.01 |
| $F2$ | 4 | 3 | 1.69 ± 0.01 |
| $F3$ | 4 | 5 | 1.71 ± 0.01 |
| $F4$ | 4 | 7 | 1.70 ± 0.01 |
| $F5$ | 4 | 9 | 1.71 ± 0.02 |
| $F6$ | 4 | 11 | 1.72 ± 0.01 |
| $AF1$ | -4 | 1 | 1.68 ± 0.02 |
| $AF2$ | -4 | 3 | 1.70 ± 0.01 |
| $AF3$ | -4 | 5 | 1.80 ± 0.02 |
| $AF4$ | -4 | 7 | 1.95 ± 0.01 |
| $AF5$ | -4 | 9 | 1.98 ± 0.02 |
| $AF6$ | -4 | 11 | 1.99 ± 0.01 |

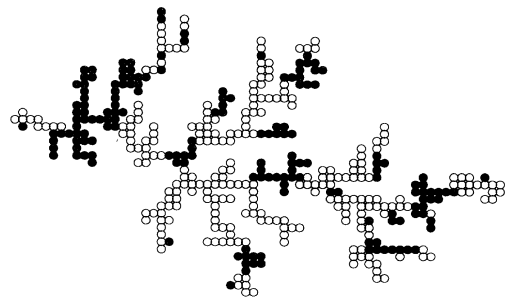


FIG. 4. A branch of a magnetically controlled diffusion-limited aggregation cluster grown from an up spin as seed and for $\beta J = +1.0$ and $\beta H = 0$.

shows a branch of a MDLA cluster grown from an up spin as seed and for $\beta J = +1.0$. Black and white dots represent up and down spins, respectively. Some domains or segments of branches are found in the same spin state which is either up or down (ferromagnetic ordering). In the following, we will study the possible domination of one species over the other during the MDLA growth process.

A. Numerical results on the line $\beta H = 0$

In order to numerically investigate the competition between the two spin species, the magnetization M of MDLA clusters have been measured during the growth for various values of βJ . The global magnetization M of one cluster is defined as the difference between the number of up and down spins in the cluster, normalized by the mass N of the cluster.

Figure 5 shows the magnetization of $N = 3000$ clusters measured for various values of the competition parameter βJ . The clusters have been grown from an up spin as seed. Each point represents an average over 80 clusters. It is seen that the magnetization m increases from zero to unity around a value $\beta J_c = 1.5 \pm 0.1$. If the clusters are grown from a down spin as seed, it is easy to check that the global magnetization falls from zero to -1 around βJ_c (not shown here). Above βJ_c , the species of the seed wins the internal competition in the cluster, while below βJ_c , the concentration of the two species are equal. Thus, a spreading phenomenon occurs around βJ_c . A similar behavior was observed in the MEM growth process [18].

Figure 6 shows the evolution of the global magnetization with the mass N of MDLA clusters on a semilog plot for various values of βJ . Each dot represents an average over 20 clusters grown from $\sigma_0 = +1$. A decrease of M with N is seen for all finite βJ values. The $M(N)$ data decrease more slowly than an exponential law for large N values. Thus, only the earlier stages of the growth are dominated by the spreading of the seed component.

The critical value βJ_c , where the magnetization presents a marked variation and, thus, where a spreading

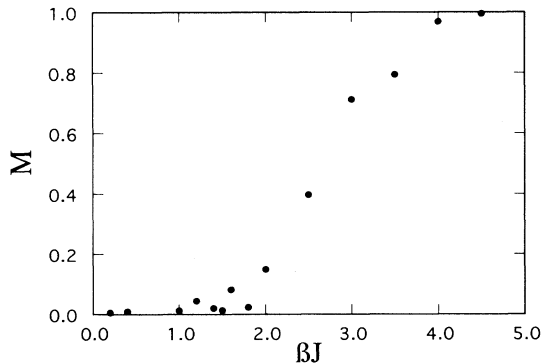


FIG. 5. Magnetization of MDLA clusters of 3000 spins grown without field from an up spin as seed as a function of the competition or coupling parameter βJ .

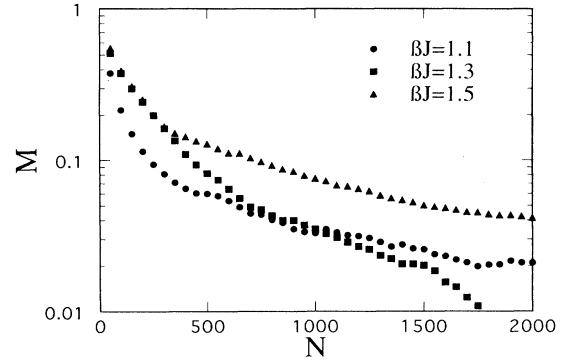


FIG. 6. The evolution of the global magnetization M with the mass N of MDLA clusters grown from an up spin as seed and for various values of the parameter βJ .

phenomenon seems to occur is found to be cluster mass dependent. The “critical transition” value βJ_c is shown in Fig. 7 as a function of the mass N of the clusters below $N = 3000$ on a semilog plot. The βJ_c value was numerically estimated to be the βJ value for which the $M(\beta J)$ curve crosses the horizontal line of equation $M = \sigma_0/20$. A logarithmic dependence

$$\beta J_c \sim \ln(N) \quad (2)$$

is found like for the magnetic Eden model [18]. The same logarithmic dependence is found if βJ_c is taken as the value at which $M(\beta J)$ has an inflection point.

The gyration radii $R_g(N)$ and $R_g^+(N)$ for, respectively, the cluster and the up component are found to be numerically equivalent, implying that $D_f = D_f^+$ for these clusters. The fractal dimension D_f of $N = 3000$ MDLA clusters are presented in Fig. 8 as a function of the coupling parameter βJ . Each dot represents an average over 80 clusters. In spite of the competition between both kinds of entities, the clusters are fractal-like because the motion of the diffusing spins is still Brownian. The fractal dimension D_f varies slowly from 1.72 ± 0.01 to 1.70 ± 0.01 with

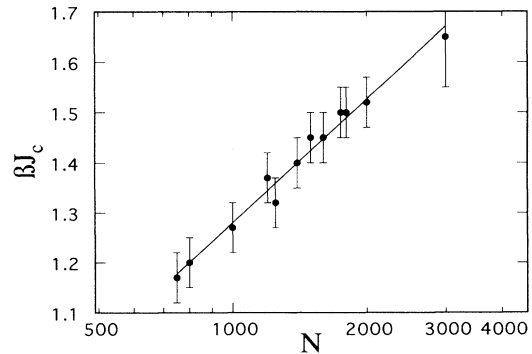


FIG. 7. The logarithmic behavior of the critical value βJ_c as a function of the size (or mass) N of the clusters.

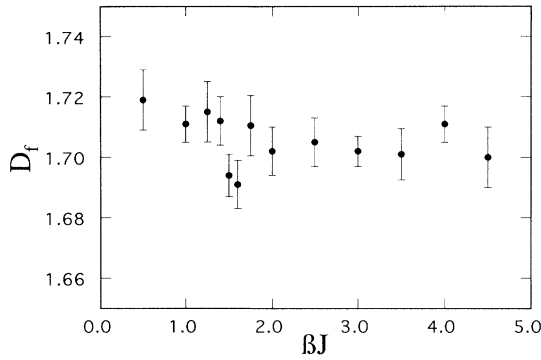


FIG. 8. Fractal dimension D_f of MDLA clusters of 3000 spins grown without field from an up spin as seed as a function of the coupling βJ .

βJ . This slight decrease was already explained in the previous section as due to βJ favoring the growth on the tip sites. A significant drop of D_f down to 1.69 ± 0.01 , is, however, clearly marked around the same magnetization critical value $\beta J_c \approx 1.5 \pm 0.1$. It was not expected that the internal magnetic “critical” phenomena occurring at βJ_c could lead to a change in the geometry of the overall cluster shape at exactly the same βJ_c for such finite-size systems.

B. Discussion

The MDLA model generates fractal-like structures similar to the branched DLA ones. As for DLA, the growth is controlled by the Brownian motion of the diffusing entities. The growth is favored on the extremities of the branches, which are better exposed to the incoming spins. Thus, the competition between both kinds of entities takes place at the tip of the branches and is only driven by the coupling parameter βJ (in absence of the external field).

During the earlier stages of the growth of a magnetically controlled DLA cluster, the competition is driven by the extension of branches of the seed species. When the size of these branches becomes greater than a characteristic “coherence” length $\xi(\beta J)$, the other spin species infects some extremity of the branches and some segment grows with a different spin species. The global magnetization M of the cluster falls rapidly to zero. A few steps later, the size of these segments reaches the characteristic length $\xi(\beta J)$ and they can become also infected. This leads to cluster branches composed of an alternance of $+1$ and -1 segments having a size of the order of ξ .

If we consider that ξ is proportional to $\exp(\beta J)$, the above considerations impose for a segment of mass N_s the following relation:

$$\xi \sim \exp(\beta J) \sim N_s^{1/\mu}. \quad (3)$$

At βJ_c , $N \sim N_s$ such that the logarithmic behavior of

$\beta J_c(N)$ found numerically in Fig. 7 is recovered. Moreover, the slope of the βJ_c vs $\ln(N)$ line in Fig. 7 gives $1/\mu$. The critical exponent μ characterizes how the size of the up or down segments scales with their mass N_s . From Eq. (3) and the slope of Fig. 7, we have found that $\mu = 1.2 \pm 0.1$ and seems to be N independent for the finite-size clusters studied so far here. This μ value is also lower than the minimum of $D_f(\beta J)$ of Fig. 8.

Thus, the MDLA clusters are fractal-like with a fractal dimension $D_f \approx 1.7$ approximately independent of βJ without field. These clusters are also divided in segments with a characteristic coherence length ξ , which scales as $\sim N_s^{1/\mu}$, where $\mu \approx 1.2$.

V. CONCLUSION

The magnetically controlled DLA (MDLA) model simulates the aggregation of particles with an internal degree of freedom, taking here, for example, two states. This generalization of DLA is geometrically, physically, and chemically relevant and leads to different competing growth processes and morphologies which are herein distributed over 24 regions of a phase diagram.

The internal properties of the clusters show that the earlier stages of the growth are dominated by the spin species of the seed but later on the various growth probabilities lead to different behaviors. This finite size process is found to imply a drastic nonexpected change of both physical and geometrical properties of the cluster during the growth history. From the spreading of both components in the clusters, we have also learned that the MDLA clusters can be divided into segments of up and down spin species having a characteristic length ξ . This characteristic length scales as a simple power law of the mass of the segments with a critical exponent $\mu \approx 1.2$.

A word is in order on the finite-size effects. The continuously varying fractal dimension with a sharp minimum at βJ_c could be considered to be an effect of large error bars due to the finiteness of the investigated systems. For moderate sticking probabilities (or large βH), the local structure seems to be compact at low N but has a DLA structure at large N . We consider that this case requires further investigations on larger systems. However, in the $\beta H = 0$ case, the range of sticking probabilities has been well investigated and the results seem to indicate a real transitionlike feature at finite N for a finite βJ . Self-similarity should strictly occur at infinite N . Our MDLA clusters are as in [9] only prefractal approximations [24]. The present work seems to indicate the interest in examining whether DLA generalizations have a crossover to self similarity for relatively small clusters and whether such a crossover occurs at the same βJ_c or N (and βH_c) values for different properties. See in this respect Ref. [14], where 100 million particle clusters were investigated. However, notwithstanding the above, finite-size systems are of interest for themselves because many natural systems are finite.

Further simulations can still be made. In particular, each boundary line of the phase diagram (see Fig. 2) should be examined. However, this leads to seven

different cases and seven plots of D_f vs βH or βJ , i.e., "several" numerical cases which are outside the scope of this paper. Finally, the relevant quantities allowing one to indicate which universality class or classes, are covered by such a MDLA and their obvious extensions should be determined through kinetic exponent evaluation [1]. This likely opens up a large field of investigations from a theoretical point of view, and also introduces much greater flexibility in modeling and understanding experimental observations.

ACKNOWLEDGMENTS

Part of this work is the continuation of some work financially supported through the SU/02/013 contract of the Impulse Program of the Belgium Federal Services for Scientific, Technical and Cultural (SSTC) Affairs. N.V. thanks the Belgium Institute for Encouragement on Scientific Research in Industry and Agriculture (IRSIA). Encouraging comments by H. E. Stanely, J. F. Gouyet, and K. Binder are appreciated.

-
- [1] H. J. Hermann, *Phys. Rep.* **136**, 153 (1986).
 [2] A. Bunde, H. J. Hermann, A. Margolina, and H. E. Stanely, *Phys. Rev. Lett.* **55**, 653 (1985).
 [3] R. F. Xiao, J. I. D. Alexander, and F. Rosenberger, *Phys. Rev. A* **38**, 2447 (1988).
 [4] M. Ausloos and J. M. Kowalski, *Phys. Rev. B* **45**, 12 830 (1992).
 [5] P. Meakin, *Phys. Rep.* **235**, 189 (1993).
 [6] L. Niemeyer, L. Pietronero, and H. J. Wiesmann, *Phys. Rev. Lett.* **52**, 1033 (1984).
 [7] M. Eden, in *Proceedings of the Fourth Berkeley Symposium on Mathematical Statistical Problems*, edited by F. Neyman (University of California Press, Berkeley, 1961), Vol. IV, p. 223.
 [8] R. Jullien and R. Botet, *J. Phys. A* **18**, 2279 (1985).
 [9] T. A. Witten and L. M. Sander, *Phys. Rev. Lett.* **47**, 1400 (1981); *Phys. Rev. B* **27**, 5686 (1983).
 [10] T. C. Halsey, *Phys. Rev. Lett.* **72**, 1228 (1994).
 [11] A. Coniglio, *Physica A* **200**, 165 (1993).
 [12] H. E. Stanely, A. Coniglio, S. Havlin, J. Lee, S. Schwarzer, and M. Wolf, *Physica A* **205**, 254 (1994).
 [13] P. Meakin, *Heterogeneous Chem. Rev.* **1**, 99 (1994).
 [14] I. Yekutieli, B. B. Mandelbrot, and H. Kaufman, *J. Phys. A* **27**, 275 (1994).
 [15] L. H. Sperling, in *Introduction to Physical Polymer Science*, 2nd ed. (Wiley, New York, 1992), p. 41.
 [16] M. Silverman and M. Simon, in *Mobile Genetic Elements*, edited by J. A. Shapiro (Academic, Orlando, 1983), p. 537.
 [17] M. Ausloos, N. Vandewalle, and R. Cloots, *Europhys. Lett.* **24**, 629 (1993).
 [18] N. Vandewalle and M. Ausloos, *Phys. Rev. E* **50**, R623 (1994).
 [19] P. Ossadnik, C.-H. Lam, and L. M. Sander, *Phys. Rev. E* **49**, R1788 (1994).
 [20] P. Meakin, *Phys. Rev. A* **27**, 604 (1983).
 [21] A. Gliozzi, A. C. Levi, M. Menessini, and E. Scalas, *Physica A* **203**, 347 (1994).
 [22] E.g., the diffusion-controlled aggregation model introduced by Meakin adds only one "sticking" probability to DLA; this does not imply any internal degree of freedom nor does it lead to any specific variety of clusters or structures, except some thickening (see Ref. [20]).
 [23] D. Dhar and R. Ramaswamy, *Phys. Rev. Lett.* **54**, 1346 (1985).
 [24] B. B. Mandelbrot, in *The Fractal Geometry of Nature* (Freeman, New York, 1982).
 [25] P. Meakin, *Prog. Solid State Chem.* **20**, 135 (1990).
 [26] P. Plischke and Z. Racz, *Phys. Rev. Lett.* **53**, 415 (1984).
 [27] L. Pietronero, A. Erzan, and C. Evertsz, *Phys. Rev. Lett.* **61**, 861 (1988).
 [28] N. Vandewalle and M. Ausloos, in *Proceedings of the Fifth Max Born Symposium, "Diffusion Processes,"* edited by A. Pekalski (Springer, Berlin, 1994).